1 **Measurement Report: Urban Ammonia and Amines in Houston, Texas**

3 Lee Tiszenkel[1], James Flynn[2], Shan-Hu Lee[1*]
4
5 [1] Department of Atmospheric and Earth Sciences, University of Alabama at Huntsville;
6 Huntsville, Alabama, USA
7 [2] Department of Earth and Atmospheric Sciences, University of Houston; Houston, Texas,
8 USA
9
10 Corresponding author (shanhu.lee@uah.edu)

Abstract. Ammonia and amines play critical roles in secondary aerosol formation, especially in urban environments. However, fast measurements of ammonia and amines in the atmosphere are very scarce. We measured ammonia and amines with a chemical ionization mass spectrometer (CIMS) at the urban center in Houston, Texas, the fourth most populated urban site in the United States, during October 2022. Ammonia concentrations were on average 4 parts per billion in volume (ppbv), while the concentration of an individual amine ranged from several parts per trillion in volume (pptv) to hundreds of pptv. These reduced nitrogen compounds were more abundant during the weekdays than on weekends and correlated with measured CO concentrations, implying they were mostly emitted from pollutant sources. Both ammonia and amines showed a distinct diurnal cycle, with higher concentrations in the warmer afternoon, indicating dominant gas-to-particle conversion processes taking place with the changing ambient temperatures. Studies have shown that dimethylamine is critical for new particle formation (NPF) in the polluted boundary layer, but currently, there are no amine emission inventories in global climate models (as opposed to ammonia). Our observations made in very polluted Houston, as well as a less polluted site (Kent, Ohio) from our previous study (You et al., 2014), indicate there is a consistent ratio of dimethylamine over ammonia at these two sites. Thus, our observations can provide a relatively constrained proxy of dimethylamine using 0.1% ammonia concentrations at polluted sites in the United States to model NPF processes.

1. Introduction

Atmospheric ammonia and amines are ubiquitous in the atmosphere, and they have been found in the gas phase, aerosol, clouds, and fog droplets (Ge et al., 2011a, b). Ammonia and amines are emitted from various natural and anthropogenic sources, such as agricultural activity, animal husbandry, vegetation, soil, waste processing, automobile traffic, power plants, and biomass burning (Ge et al., 2011a). Ammonia and amines often share the same emission sources. In general, ambient concentrations of ammonia are at the parts per billion in volume (ppbv) range, and amines are approximately two to three orders of magnitude lower than ammonia concentrations. Ambient concentrations of ammonia and amines vary rapidly due to emission, gas-to-particle conversion, and wet deposition processes (You et al., 2014; Yu and Lee, 2012).

Laboratory studies have shown that ammonia and amines play key roles in new particle formation (NPF) as they can stabilize sulfuric acid clusters (Yu et al., 2012; Almeida et al., 2013; Lehtipalo et al., 2018; Xiao et al., 2021; Glasoe et al., 2015; Jen et al., 2016). In particular, dimethylamine can have a profound effect on atmospheric processes even at the pptv level (Almeida et al., 2013; Glasoe et al., 2015). Field observations show that ammonia and amines are associated with NPF events in Chinese megacities (Yao et al., 2016; Yan et al., 2021; Cai et al., 2021; Cai et al., 2023), urban areas in the United States (Jen et al., 2016; Smith et al., 2010), European cities (Brean et al., 2020), a high altitude site (Bianchi et al., 2016), and the Arctic and Antarctic (Beck et al., 2021; Brean et al., 2021; Jokinen et al.; Köllner et al., 2017). However, global models cannot simulate urban NPF processes currently because of the lack of amine emission inventories in models.

51 Ammonia and amines also contribute to secondary organic aerosol (SOA) formation by
52 condensation of oxidation products formed by reactions with ozone, OH, or NO_3 radicals and
53 produce light-absorbing particles (Erupe et al., 2010; Malloy et al., 2009; Silva et al., 2008;
54 Nielsen, 2016; Nielsen et al., 2012; Qiu and Zhang, 2013). As a result, reducing ammonia
55 emissions has been identified as a cost-effective way to mitigate ambient fine particle
56 concentrations (Gu et al., 2021).

57 Fast-response measurements of ammonia and amines at atmospheric concentrations are very
58 challenging (Lee, 2022), although such measurements are necessary because these reduced
59 nitrogen compounds have relatively short atmospheric lifetimes (Nielsen et al., 2012). Previously,
60 (Schwab et al., 2007) made an intercomparison of six different ammonia detection methods in the
61 laboratory and found a large variance in the measured concentrations and vastly different response
62 times (over several hours) within different instruments. Difficulties in the detection of base
63 compounds also arise because these "sticky" compounds can rapidly adsorb and desorb on/from
64 the surfaces of sampling inlets to cause background signals that vary depending on ambient
65 concentrations, air humidity, and other atmospheric conditions. Thus frequent, in situ
66 measurements of instrument background signals using proper zero gases are required, especially
67 for field observations with rapidly changing ambient concentrations of base compounds.

68 Chemical ionization mass spectrometers (CIMS) using ion reagents such as protonated ethanol,
69 acetone, and water ions can detect ammonia and amines in the atmosphere with fast response
70 (Nowak et al., 2006; Benson et al., 2010; Yu and Lee, 2012 ; Hanson et al., 2011; Jen et al., 2016;
71 Nowak et al., 2010). As summarized in Table 1, CIMS technique has been used for the detection
72 of ambient ammonia and amines at a polluted site in Ohio (You et al., 2014; Yu and Lee, 2012),
73 a rural Alabama forest (You et al., 2014), and polluted urban sites in China (Zheng et al., 2015;
74 Wang et al., 2020a; Wang et al., 2016; Zhu et al., 2022). As shown in Table 1, there are even fewer
75 studies that simultaneously measured ammonia and amines. The CIMS using ethanol reagent can
76 measure amines at or below single-digit pptv concentrations with a time response of 1 minute and
77 measure simultaneously amines and ammonia (You et al., 2014; Yu and Lee, 2012 ; Erupe et al.,
78 2011; Benson et al., 2010). The CIMS using protonated water ions (i.e., proton-transfer chemical
79 ionization mass spectrometer, PTR-CIMS) can measure mono- and di-amines (Hanson et al., 2011;
80 Jen et al., 2016). Using a high-resolution time-of-flight (HR-TOF) detector coupled to CIMS (HR-
81 TOF CIMS) (with ethanol reagent), (Yao et al., 2016) measured various amines and amides in
82 Shanghai. However, isomers of amines were still not resolved in the detection; for example, the
83 measured C2-amines still contained dimethylamine and ethylamine. Thus, a major disadvantage
84 of a mass spectrometer (regardless of mass resolution) is the inability to resolve/identify isomers.
85 To resolve isomers, tandem MS/MS analysis or an additional independent separation method (such
86 as chromatography) coupled to the mass spectrometer is necessary.

87 In situ measurements of ammonia have been made in various atmospheric environments also
88 with optical techniques such as open-path absorption (Miller et al., 2014), closed-path absorption
89 (Griffith and Galle, 2000; Ellis et al., 2010; Mcmanus et al., 2010; Leen et al., 2013; Pollack et al.,
90 2019), cavity ring-down spectroscopy (Martin et al., 2016), and photoacoustic spectroscopy

(Pushkarsky et al., 2002). These fast-response optical techniques were used for flux and aircraft measurements of ammonia.

We measured ammonia and C1-C6 amines with an ethanol CIMS in October 2022 at the urban center in Houston, Texas. Houston is the fourth most populated urban center in the U.S. and contains a diverse range of pollutant emissions from urban activity, traffic, ship channels, oil production, marine air masses, and agricultural activity. The primary goal of these measurements is to quantify ammonia and C1-C6 amines in an urban setting and identify the atmospheric conditions that affect their abundance. The study is amongst very few observations of ammonia and amines at highly polluted urban sites in the U.S. We also compare observations in Houston with previous measurements taken with the same instrument in Kent, Ohio (less polluted) (You et al., 2014) and establish a quantitative relationship between ammonia and dimethylamine in a different range of polluted conditions. This relationship will allow global models to simulate urban NPF processes using the existing ammonia emission inventories.

2. Methods
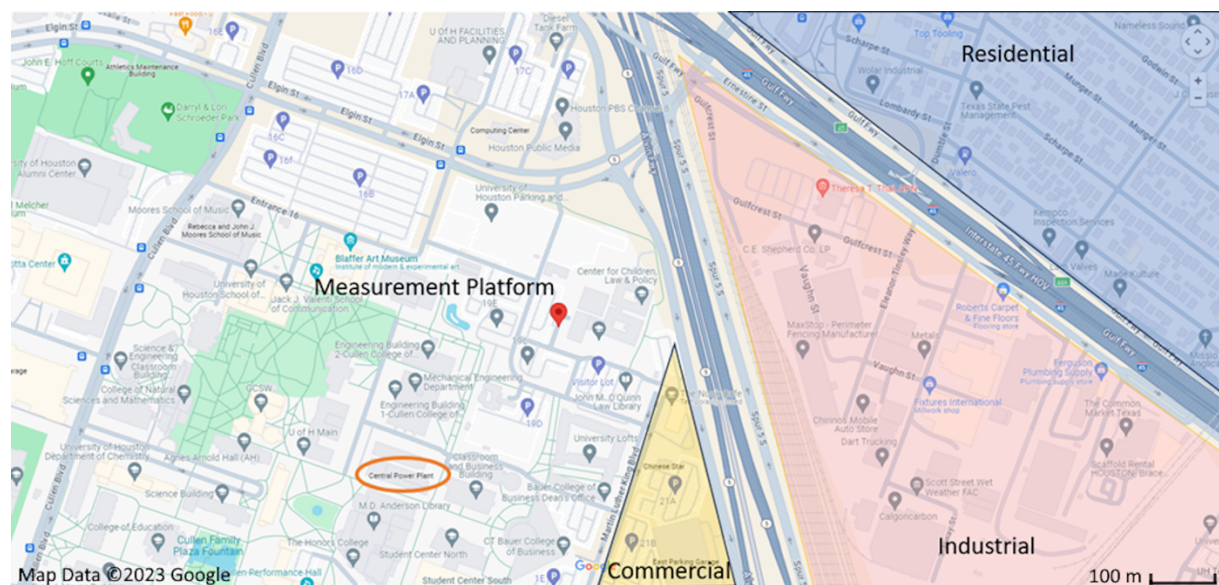
Figure 1. Location of the measurement platform, indicated by a red pin in the center of the map. Nearby commercial, industrial, and residential areas are labeled by yellow, red, and blue shaded sections, respectively. The nearby University of Houston power plant is circled in orange to the southwest of the measurement platform. The map of the greater Houston urban area, as well as the satellite view of the nearby vicinity of the measurement site, are shown in Figure S1.

The field observation took place in Houston continuously from the 8th to the 27th of October in 2022. Measurements were made at a stationary platform located on the campus of the University of Houston (29.72° N, 95.34° W) ~2.5 km from central downtown Houston. Maps of the measurement site (Figures 1 and S1). The measurement platform was located ~5 m from an active

119 parking lot, ~200 m from a low-traffic road, ~300 m from a high-traffic thoroughfare, and ~500 m
120 from an interstate highway. The immediate vicinity of the site was the University of Houston
121 campus, containing classroom buildings, dormitories, facilities services, and dining halls. Nearby
122 to the southeast of the site were several restaurants as well as an industrial park containing sites of
123 chemical supply companies, construction, machining services, and automobile shops. The site was
124 surrounded by residential areas to the south, northeast, and west. The city center and highest
125 population densities were to the northeast of the measurement site.
126
127 The ethanol CIMS instrument used has been described in detail previously (Benson et al.,
128 2010; You et al., 2014; Yu and Lee, 2012). The CIMS draws 10 standard liter per minute (slpm)
129 of sample air into a low-pressure ion-molecule region (about 2,000 Pa) where the flow mixes with
130 a pure nitrogen flow with a 2 slpm through a stainless-steel vessel of 200-proof ethanol, followed
131 by a ^{210}Po radiation source. Ammonia and amines were detected with the following ion-molecule
132 reactions based on (Erupe et al., 2011), (Yu and Lee, 2012), and (Nowak et al., 2006):
133 $$(C_2H_5OH)_nH^+ + NH_3 \rightarrow (C_2H_5OH)_{n-1}NH_4^+ + C_2H_5OH$$
134 $$(C_2H_5OH)_nH^+ + B \rightarrow BH^+ + nC_2H_5OH$$
135 Here, "B" refers to amines, and "n" is the number of reagent ions measured by the CIMS (n=1-3).
136 The $(C_2H_5OH)_2H^+$ (m/z = 93) peak was the highest among the three reagent ions (m/z = 47, 93,
137 and 140). As shown in Figure S2, the production ions of amines were protonated ions: C1-amine
138 (m/z = 32), C2 (m/z = 46), C3 (m/z = 60), C4 (m/z = 74), C5 (m/z = 88), and C6 (m/z = 102).
139 Ammonia product ions were NH_4^+ (m/z = 18, higher peak) and $(C_2H_5OH)NH_4^+$ (m/z = 64, lower
140 peak); these two ions were strongly correlated to each other during the ammonia calibration and
141 ambient measurements, indicating they represent ammonia signals.
142 To obtain a background signal, the CIMS is operated with 10 minutes of sampling followed
143 by 10 minutes of background measurements. Figure S2 shows the main reagent and base
144 compound product ions during the switching between ambient and background measurements.
145 Background measurements were taken by switching a 3-way valve to supply the inlet with a flow
146 of zero air through a silicon phosphate medium (Pan Tech, Texas) to scrub ammonia and amines.
147 The reagent signal was taken as the sum of three ethanol reagent ions. Reagent ion signals were
148 typically around 400 kHz with less than 10 % difference between ambient and background
149 measurement modes. Ammonia and amine concentrations were calculated by the difference
150 between the ambient and background signals normalized to 1,000,000 Hz of reagent ion signal
151 multiplied by a calibration factor. Calibration of the instrument was carried out with diluted
152 ammonia in nitrogen and permeation tubes of methylamine, dimethylamine, trimethylamine,
153 diethylamine, and diisopropylamine (Kin-tek, USA). Due to the difficulty of obtaining a
154 calibration standard, C5 amines were assumed to have the same sensitivity as C6 amines. The
155 calibration factors for each compound and detection limits were found to be similar to the results
156 from the calibration of the instrument by (You et al., 2014) (Table S1), over a period of nearly 10
157 years, demonstrating an excellent reproducibility in the instrument performance. The time
158 response of the CIMS instrument to ammonia and amines is defined as where the signal stabilizes

159   at its "double e-folded" concentration of $1/e^2$ during the calibration. Average response times for
160   ammonia and amines were smaller than 1 minute. For each 10-minute cycle of background and
161   measurement, the first two minutes of each background/measurement cycle were excluded from
162   the data analysis to allow the instrument to reach a steady concentration.

163   The uncertainty in the CIMS included error in the permeation sources, which ranged from 2%
164   to 5% depending on the compound. The permeation sources were diluted in two stages using flow
165   controllers that each had uncertainties of 1.5%. Total error in the calibration of the CIMS was
166   6.7%. Overall uncertainty in the CIMS was 30%, accounting for calibration error, variability of
167   ion signals, and inlet losses.

168   Meteorological data was measured concurrently on the platform by a Vaisala HMP-45c for
169   temperature and relative humidity, and a RM Young 05305 wind speed and direction sensor.
170   Additionally, CO and NO_x ($NO+NO_2$) were measured with Thermo 48c and Thermo 42c-TL,
171   respectively. These measurements were provided by the University of Houston. The uncertainty
172   in trace gas (CO and NO_x) measurements arises from instrumental uncertainty in the Thermo 48c
173   CO analyzer and Thermo 42c-TL NO_x analyzer. Zero correction was performed on this instrument
174   daily by switching to a flow of zero air. The typical uncertainty of each of these instruments was
175   5%.

176
177
178   **3. Results and Discussion**
179

180
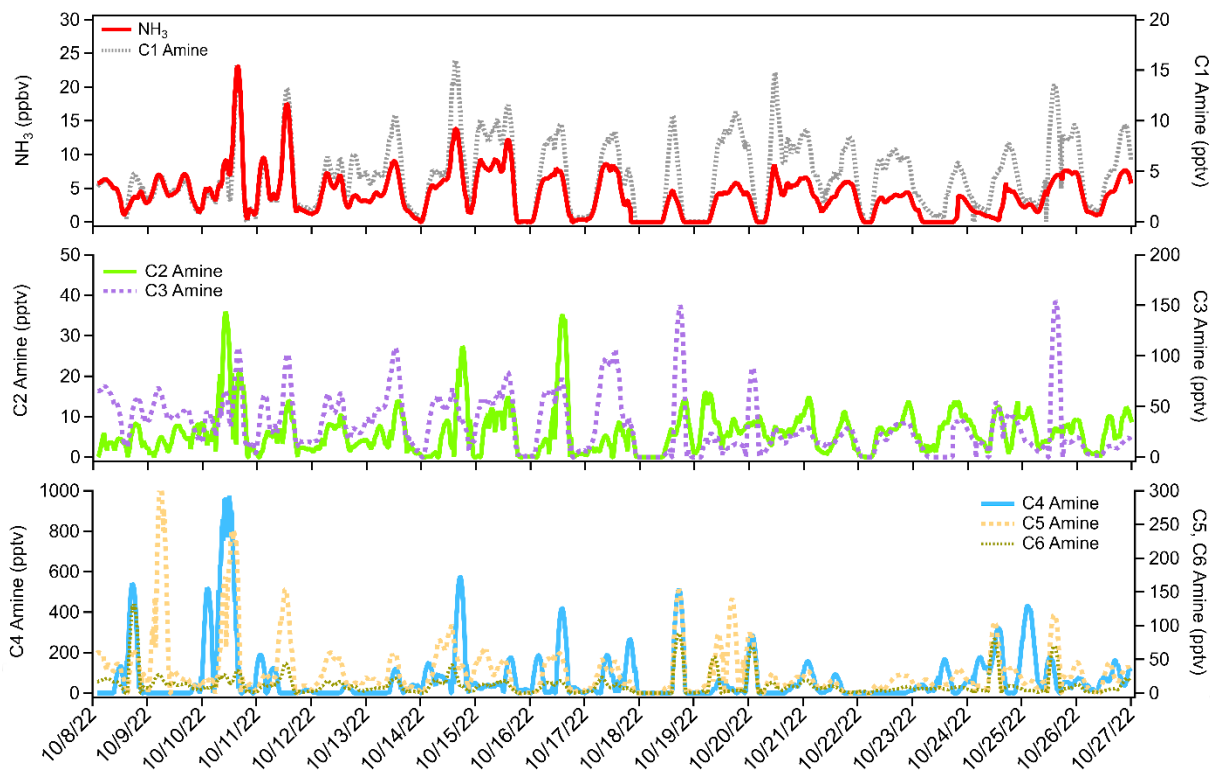
Figure 2. Time series of ammonia and C1-C6 amines observed at the urban center in Houston, Texas, in October 2022.

The time series of ammonia and amines during the ambient measurement period is shown in Figure 2. The average ammonia concentration during the measurement campaign was 4 ppbv with several short-term spikes above 10 ppbv and one occasion when the concentration exceeded 20 ppbv. Concentrations of C1 amine averaged 4 pptv with several spikes up to 15 pptv. Average C2 amine concentrations were 6 pptv with frequent but brief periods of concentrations more than 10 pptv. Average C3 amine concentrations were 31 pptv with brief increases in concentration above 100 pptv. C4 amine was the most abundant amine observed during the measurement period with an average concentration of 79 pptv with spikes in concentration into the hundreds of pptv. Average C5 and C6 amine concentrations were 33 and 12 pptv, respectively. These concentrations in Houston were generally consistent with concentrations measured in other urban sites (Table 1). Previous CIMS ammonia measurements from aircraft flights above Houston observed similar baseline concentrations of ammonia (0.2-3 ppbv) with brief spikes in concentration (up to 80 ppbv) associated with agricultural or industrial activity (Nowak et al., 2010). Additionally, ammonia concentrations of similar magnitude to the high spikes in concentration observed in this study have been reported in Shanghai (Xiao et al., 2015) as well as an urban site in Romania (Petrus et al., 2022), with high ammonia concentrations corresponding to high temperatures and high traffic activity. Long-term measurements taken in Nanjing with a cavity ring-down spectrometer also showed an average ammonia concentration of 12 ppbv (Liu et al., 2024). Measurements of amines in Atlanta, Georgia showed <1 to 3 pptv concentrations of C1 and C2 amines, and C3 and C6 amines up to 15-25 pptv (Hanson et al., 2011). Yao et al. (Yao et al., 2016) measured amines at the level of pptv or sub-pptv, e.g., C2 amines of 3.9 ± 1.2 pptv, in urban Shanghai during the summer. It is possible that measured concentrations of amines measured here contain some interference from amides formed from oxidation of emitted amines. The CIMS does not have sufficient resolving power to separate trimethylamine (m/z 59.11) from acetamide (m/z 59.07), for example. Therefore, these amine concentrations represent an upper limit of amine concentrations (assuming all of the detected signal is due to the presence of amines). However, (Yao et al., 2016) measured amide concentrations in urban Shanghai in the tens to hundreds of pptv, while C1-C2 amine concentrations in Shanghai were similar to Houston observations reported here. Considering the consistency between amine measurements at these two urban locations, it is likely that interference from amides in the CIMS was minimal for C1 and C2 amines. The discrepancies between these two urban areas become more pronounced for C3-C6 amines (Table 1), which makes amide interference a possible explanation for elevated concentrations of C3 amines and above.

217
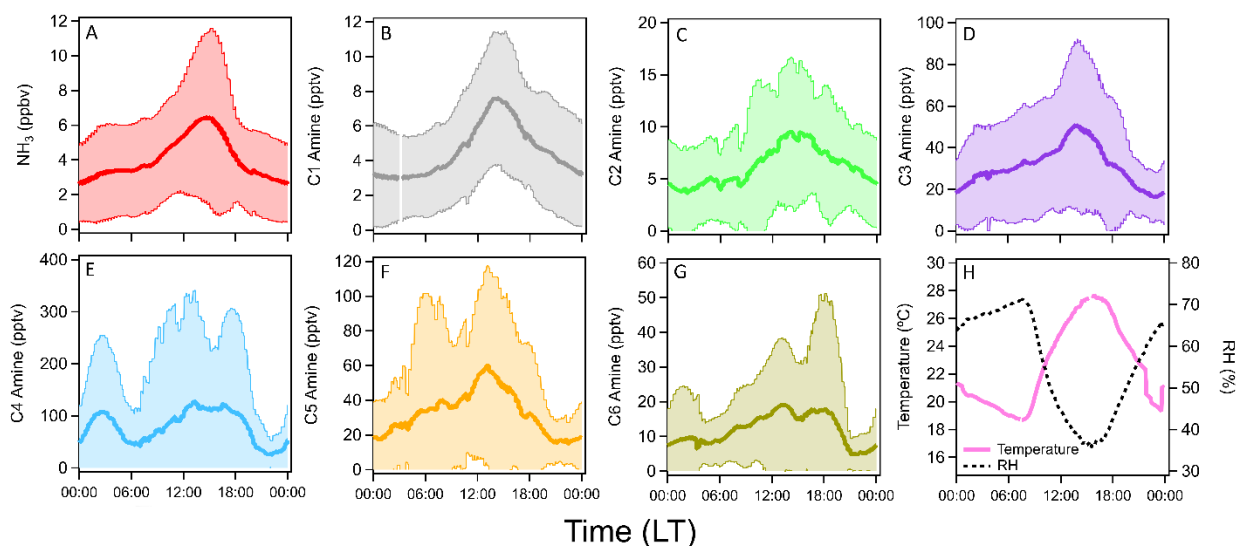
Figure 3. Averaged diurnal cycles of (a) ammonia, (b-g) C1-C6 amines, (h) temperature, and RH in Houston, Texas, during the observation period (19 days continuously). Shaded areas indicate 1 standard deviation from the mean values of observation data.

Figure 3 shows the averaged diurnal concentrations of ammonia and amines during the observation period. Ammonia and amines had a diurnal cycle with peak concentrations in the afternoon with higher ambient temperatures. Generally, ammonia and amines correlated with one another throughout the measurement campaign, while C1-C3 amines showed the highest correlation with ammonia. Peak concentrations of all compounds corresponded with the high temperature of the day at around 3 pm local time. This was especially pronounced for ammonia, C1 and C3 amines. The relationships between ammonia and amines and temperature are shown in Figure 4. Ammonia had the strongest correlation with temperature, and the relationship fit an exponential parameterization, as the following:

$$[NH_3] = 2.85 + 9.66 \times 10^{15} \, e^{-\frac{10619}{T}}$$

Amines generally showed linear relationships with temperature, with C3 and C4 amines displaying the strongest relationships. C3 amines increased by 2.3 pptv per °C ($r^2 = 0.86$) and C4 by 2.9 pptv per °C ($r^2 = 0.65$). C5 and C6 amines were also moderately correlated with temperature, increasing by 1.2 pptv per °C and 0.5 pptv per °C, respectively ($r^2 = 0.60$ for both C5 and C6). On the other hand, the correlation of C1 and C2 amines with temperature were weaker: C1 only increased by 0.1 pptv per °C with almost no correlation ($r^2 = 0.22$), and C2 increased by 0.8 pptv per °C ($r^2 = 0.50$). The temperature dependence of ammonia and amines was previously observed in a rural forest in Alabama by (You et al., 2014), which attributed this partially to particle-to-gas conversion of ammonia and amine containing particles at elevated temperatures. The temperature dependence could also be due to higher emissions at higher temperatures. The temperature dependence of ammonia and amines has been observed at other urban, suburban and rural locations such as Kent,

Ohio (You et al., 2014), Atlanta (Hanson et al., 2011), Delaware (Freshour et al., 2014), the Southern Great Plains (Freshour et al., 2014), and rural central Germany (Kürten et al., 2016).
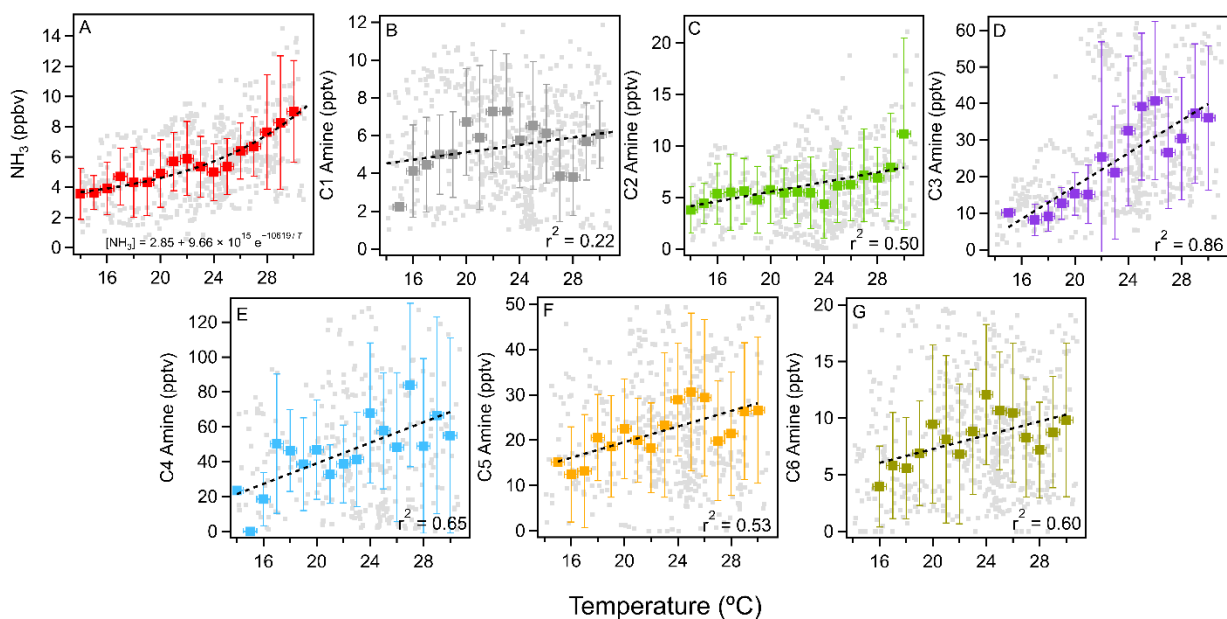
Figure 4. Temperature dependence of (a) ammonia and (b-g) C1-C6 amines measured in Houston. Vertical bars indicate 1 standard deviation from the mean values of observation data. Binned temperatures are shown in colored squares, 1-minute averaged data is shown in gray squares. Horizontal bars indicate bin width. Black dashed lines indicate exponential fit for ammonia and linear fits for amines.

Anthropogenic pollutants such as CO and NO_x and CO can serve as tracers for industrial and traffic activities. Ammonia and amines in general showed a positive correlation with CO, with the exception of C3 amines (Figure 5). As ammonia, amines, and CO can be traced to traffic or industrial emissions, the positive relationship between these compounds implies that these base compounds were emitted from pollutant sources. Unlike with CO, there was a negative correlation with NO_x (Figure S3). This lack of a strong correlation between NO_x and ammonia was previously observed in Nanjing where a strong reduction in NO_x concentration during COVID-19 lockdown periods was not accompanied by an equivalent reduction in ammonia concentrations (Liu et al., 2024). This may indicate some unique emission sources for ammonia and amines that do not co-emit NO_x.
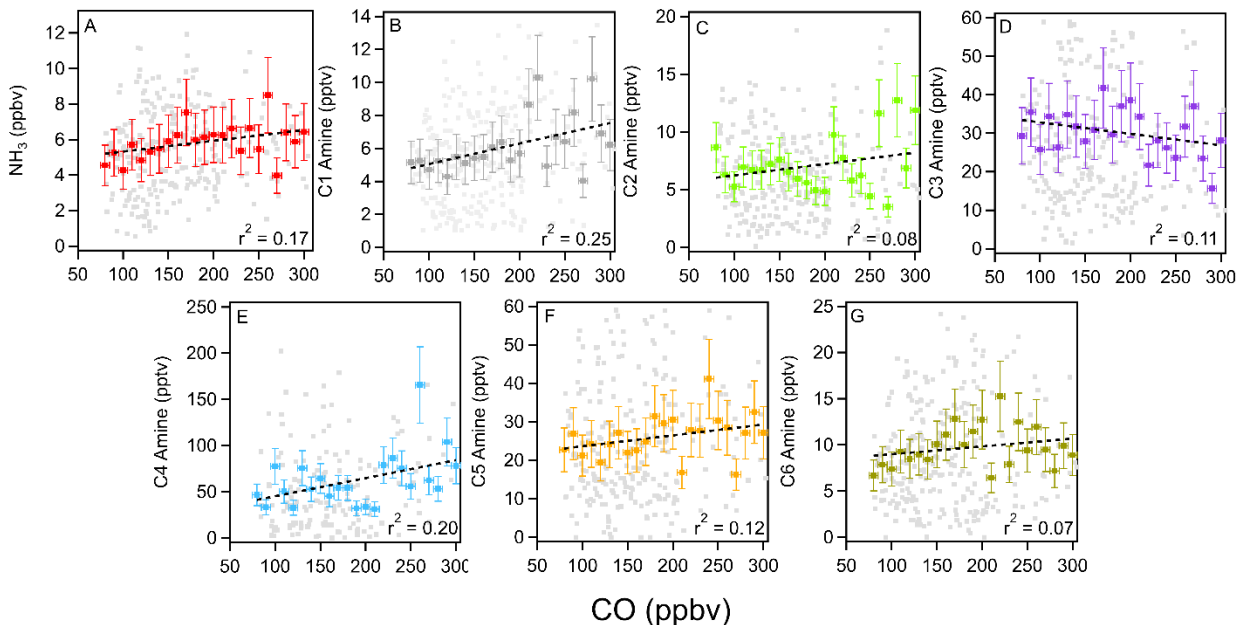
Figure 5. Correlation between ammonia (a) and C1-C6 amines (b-g) with the collocated CO concentrations during the measurement campaign. Binned CO concentrations are shown in colored squares, 5-minute averaged data shown in gray squares. Vertical bars indicate 1 standard deviation from the mean values of observation data. Horizontal bars indicate bin widths. Black dashed lines indicate linear fits.

Wind speed and direction can help to identify local sources of ammonia and amines near the measurement site. Figures 6 and S4 show the correlation of ammonia and amines with wind speeds and direction throughout the observation period. Consistent between all base compounds is the high concentration coming from the southeast. This is the direction of the interstate highway, industrial areas, and train yards (Figures 1 and S1). Ammonia and most amines also have a pronounced source from the northwest – this is the direction of downtown Houston, where population density is highest. Except for C2 and C4 amines, the observed ammonia and amines in Houston were higher during periods of low wind speeds. The abundant C2 and C4 at high wind speeds may suggest that C2 and C4 amines were transported from more distant sources.

Figure S5 shows the average diurnal cycle of ammonia and amines on weekdays as opposed to weekends. Except for C2 and C4 amines, there was a clear decrease in concentrations during weekends during the afternoon peak. Weekends saw much less traffic and activity on the University of Houston campus. During this observation period, ambient temperatures were higher during the weekends, which would increase emissions. Therefore, the differences in weekdays vs. weekends indicate that amines and ammonia were indeed emitted from traffic and industrial activities. Lower average amine concentrations on weekends were also observed during mobile measurements in Yangtze River Delta cities (Chang et al., 2022).
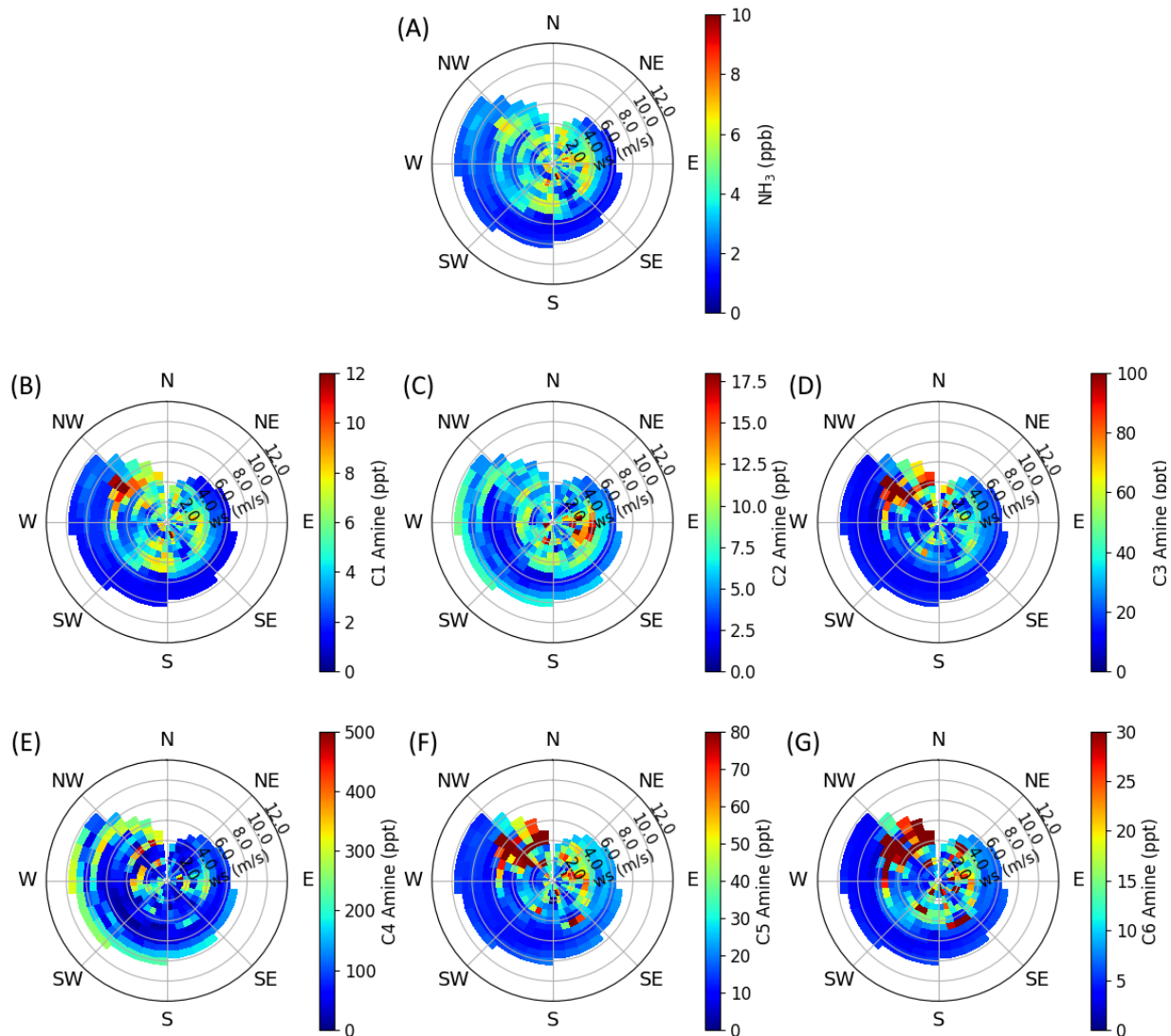
Figure 6. Wind rose plots of (a) ammonia and (b-g) C1-C6 amines observed in urban Houston. The color scale indicates concentration, and radial intensity shows wind speed.

4. Atmospheric Implications

Field observations show that sulfuric acid and amines are responsible for aerosol nucleation (Yao et al., 2016; Yan et al., 2021; Cai et al., 2021; Cai et al., 2023; Jen et al., 2016; Smith et al., 2010; Brean et al., 2020), however, currently, global models do not have amine emission inventories. Figure 7 shows the correlation of ammonia with C1-C6 amines measured during this campaign. This figure also includes that data obtained with the same instrument in Kent, Ohio, (You et al., 2014). It is clear from this figure that concentrations of ammonia, C1, C2, C3, C5, and C6 amines were positively correlated with one another throughout the study: r^2 values for the correlation between ammonia and amines were 0.61 for C1, 0.42 for C2, 0.47 for C3, 0.26 for C5

303 and 0.88 for C6. These relationships imply that these compounds are mostly co-emitted from
304 similar sources and undergo similar atmospheric transport. C4 amines showed no correlation with
305 ammonia and lower-mass amines – the r^2 value for C4 vs. NH_3 was 0.048. This indicates a unique
306 source for C4 amines, consistent with both elevated C4 concentrations at high wind speeds and
307 higher weekend C4 concentrations as discussed previously. Correlations of C1-C3 amines
308 concentrations, taken from the linear fits of the plots shown in Figure 7, were approximately
309 equivalent to 1.1×10^{-3} [NH_3], 1.4×10^{-3} [NH_3], and 8.4×10^{-3} [NH_3], respectively. C5 and C6
310 amine concentrations were 1.9×10^{-2} [NH_3] and 3.5×10^{-3} [NH_3], respectively (Table S2). From
311 these results, we propose that global modelers use 0.1 % of the ammonia concentration as a proxy
312 of dimethylamine to simulate urban NPF processes. However, this recommendation comes with
313 the caveat that measured C2 amines may include dimethylamine as well as ethylamine due to the
314 inability of mass spectrometry to resolve isomers. Therefore, this correlation represents only the
315 upper bound of dimethylamine concentrations.

316
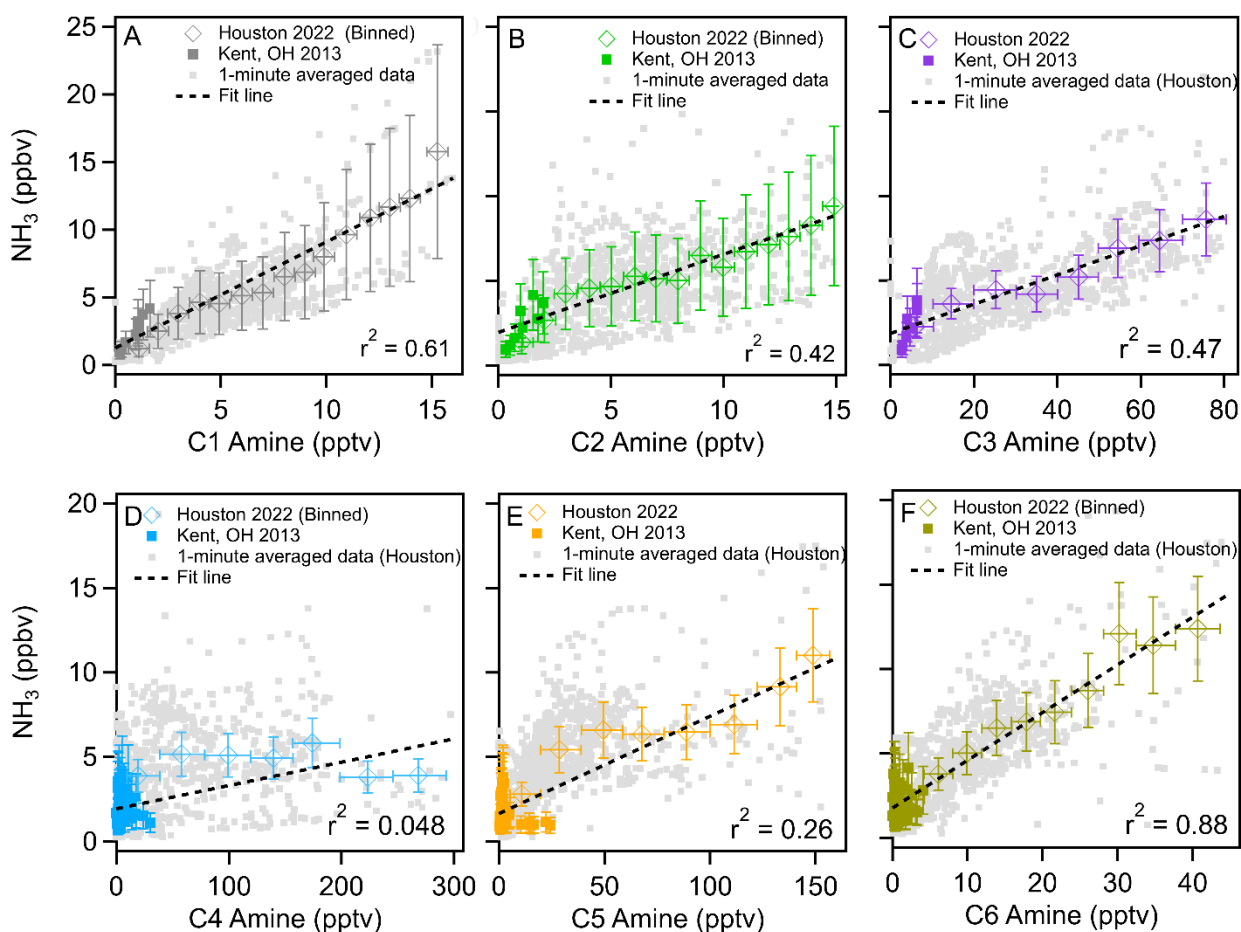
317

318 **Figure 7.** Correlations of C1-C6 amines with ammonia throughout the observation period in
319 Houston (diamonds) and Kent, OH (squares) as reported by (You et al., 2014). Binned
320 concentrations are shown in colored squares, 1-minute averaged data from Houston are shown in

gray squares. Vertical bars indicate one standard deviation from the mean values of observation data. Horizontal bars indicate bin widths. Black dashed lines indicate linear fits of the combined data from Kent and Houston.

From these observations made in very polluted Houston and less polluted Kent, we propose that at the polluted sites in the United States, dimethylamine concentrations can be estimated using the proxy, 0.1% ammonia concentrations. The caveat of this proxy is that it is based on only two locations in the United States and did not consider different emission sectors. There has been so far only one attempt to use quantify the aerosol nucleation processes using sulfuric acid and dimethylamine in the global model by Zhao et al. (Zhao et al., 2024) and they concluded that this nucleation process is dominant globally in polluted boundary layer, from China, India, Europe to United States. In this cited study the authors used the proxy of dimethylamine using ammonia concentrations, for example, dimethylamine/ammonia ratio of 0.0070, 0.0018, and 0.0100, for chemical industrial, other industrial, and residential sources; these proxies were derived by Mao et al. (Mao et al., 2018) based on the measurement made in Nanjing (Zheng et al., 2015). Our observations indicate that (Zhao et al., 2024) likely overestimated dimethylamine concentrations for polluted sites in the United States overall, and thus overpredicted nucleation rates as well. Thus, our results can provide more constrained proxy for polluted sites in the United States for future modeling studies.

5. Conclusions

Our observations in urban Houston show that ammonia and amines generally followed a clear diurnal cycle, peaking in the early afternoon when the ambient temperature was highest during the day. We found a correlation between ammonia/amines and ambient temperature. The diurnal cycles and temperature dependence of these compounds are consistent with (You et al., 2014) which showed that the gas-to-particle conversion contributes to the temperature dependence. To verify this process, the chemical composition of particle is needed, but particle measurements were not available during the present study. Additionally, the observed temperature dependence could be due to increased emissions of ammonia and amines from biogenic and anthropogenic sources. On the other hand, photochemical aging that occurs typically during the higher solar flux can also reduce the gas phase amines at the noontime; thus, photochemical aging was unlikely the main driving factor to produce higher concentrations of amines around noon.

High concentrations of ammonia and amines were correlated with local air masses from densely populated areas and areas of high traffic, industry, and other human activity. This suggests that most ammonia and amines measured in Houston originated from pollutant sources, consistent with the correlation observed with CO concentrations. There was also a clear increase in ammonia and amines on days with more human activity as shown by the results of concentrations on weekends vs weekdays. We observed a consistent relationship between ammonia and amines during our measurement campaign as well as with observations in less densely populated Kent, Ohio, suggesting that it is reasonable to parameterize amine emission inventories based on existing ammonia inventories to simulate urban NPF processes. However, as the CIMS is incapable of

resolving amides or isomers, this parameterization is only capable of representing the upper bounds of amines. Further work involving instrumentation capable of isomer resolution such as tandem MS/MS or chromatographic separation is needed to determine typical isomer ratios of amines for more accurate parameterizations.

Measuring ammonia and amines in the atmosphere is one of the most challenging areas in the development of atmospheric analytical instruments (Lee, 2022; Lee et al., 2019). The CIMS used in this campaign is currently one of the few instruments in the world that is capable of simultaneous measurements of ammonia and amines at atmospherically relevant detection limits and timescales. Very importantly, our CIMS, despite its relatively low mass resolution, has measured ammonia and amines at various atmospheric conditions, ranging from the rural forests (You et al., 2014; Kanawade et al., 2014), a relatively less polluted site (Yu and Lee, 2012 ; You et al., 2014; Erupe et al., 2010), to the extremely polluted urban environment (this study), with consistent instrument sensitivities over the decade; to our knowledge, this is the only instrument that demonstrated such consistency in the performance. Studies have shown that the co-presence of ammonia and amines can enhance sulfuric acid nucleation rates compared to ammonia alone (Yu et al., 2012; Glasoe et al., 2015; Myllys et al., 2019). From this perspective, simultaneous measurements of ammonia and amines will be required for the correct prediction of NPF processes in the atmosphere. Measurements of ammonia and amines with comprehensive calibration as shown in the present study are very even rarer, but such measurements are needed for mitigating urban air quality problems and the health effects of ultrafine particles.

Author Contributions

SHL designed the research; LT and SHL performed measurements; JF provided the measurement platform as well as the trace gas and meteorology data; LT and SHL wrote the manuscript.

Competing interests

The authors declare that they have no conflict of interest.

Data/code availability

The data used in this study are available at the Zenodo repository site, DOI: 10.5281/zenodo.11086677. The codes used in this study will be available at the request to the corresponding author (shanhu.lee@uah.edu).

Acknowledgements

We acknowledge funding support from National Science Foundation (grant numbers 2209722, 2117389, and 2107916) and Texas Commission on Environmental Quality (grant number 582-22-31535-018).

Table 1. Ammonia and amine measurements with CIMS at various locations reported in the literature. DL, detection limit of each instrument.

Location	NH$_3$ (ppbv)	C1 Amine (pptv)	C2 Amine (pptv)	C3 Amine (pptv)	C4 Amine (pptv)	C5 Amine (pptv)	C6 Amine (pptv)
Rural Alabama Forest (You et al., 2014)*	Up to 1-2	< DL	< DL	1 - 10	< DL	< DL	< DL
Kent, Ohio (You et al., 2014)*	Up to 6	1 – 4	< DL	5 - 10	10 - 50	10 - 100	< DL
Kent, Ohio (Yu and Lee, 2012)*	0.5 ± 0.26	-	8 ± 3	16 ± 7	-	-	-
Atlanta, Georgia (Hanson et al., 2011)†	-	< 1	3	4 – 15	25	-	-
Lewes, Delaware (Freshour et al., 2014)†	0.8	5	28	6	150	1	2
Lamont, Oklahoma (Freshour et al., 2014)†	0.9	4	14	35	150	98	20
Minneapolis, Minnesota (Freshour et al., 2014)†	1.8	4	42	19	14	20	5
Shanghai (Yao et al., 2016)‡	-	3.9 ± 1.2	6.6 ± 1.2	0.4 ± 0.1	3.6 ± 1.0	0.7 ± 0.3	1.8 ± 0.8
Nanjing (Zheng et al., 2015)‡	1.7 ± 2.3	7.2 ± 7.4 (C1 + C2 + C3)			-	-	-
Wangdu	-	-	14.6 ± 14.9	-	-	-	-

(Wang et al., 2020b)§							
Beijing (Zhu et al., 2022)‡	2.8 ± 2.0	5.2 ± 4.3 (C1 + C2 + C3)	-	-	-		
Houston, TX (This study)*	4 ± 1	4 ± 2	6 ± 2	31 ± 9	79 ± 30	33 ± 12	12 ± 4

* CIMS with ethanol reagent

† Proton-transfer chemical ionization mass spectrometer (PTR-CIMS)

‡ High-resolution time of flight chemical ionization mass spectrometer (HR-TOF CIMS) with ethanol reagent

§ Vocus proton transfer time-of-flight mass spectrometer (PTR-TOF MS)

References

Almeida, J., Schobesberger, S., Kürten, A., Ortega, I. K., Kupiainen-Määttä, O., Praplan, A. P.,
    Adamov, A., Amorim, A., Bianchi, F., Breitenlechner, M., David, A., Dommen, J.,
    Donahue, N. M., Downard, A., Dunne, E., Duplissy, J., Ehrhart, S., Flagan, R. C.,
    Franchin, A., Guida, R., Hakala, J., Hansel, A., Heinritzi, M., Henschel, H., Jokinen, T.,
    Junninen, H., Kajos, M., Kangasluoma, J., Keskinen, H., Kupc, A., Kurtén, T., Kvashin,
    A. N., Laaksonen, A., Lehtipalo, K., Leiminger, M., Leppä, J., Loukonen, V.,
    Makhmutov, V., Mathot, S., McGrath, M. J., Nieminen, T., Olenius, T., Onnela, A.,
    Petäjä, T., Riccobono, F., Riipinen, I., Rissanen, M., Rondo, L., Ruuskanen, T., Santos,
    F. D., Sarnela, N., Schallhart, S., Schnitzhofer, R., Seinfeld, J. H., Simon, M., Sipilä, M.,
    Stozhkov, Y., Stratmann, F., Tomé, A., Tröstl, J., Tsagkogeorgas, G., Vaattovaara, P.,
    Viisanen, Y., Virtanen, A., Vrtala, A., Wagner, P. E., Weingartner, E., Wex, H.,
    Williamson, C., Wimmer, D., Ye, P., Yli-Juuti, T., Carslaw, K. S., Kulmala, M., Curtius,
    J., Baltensperger, U., Worsnop, D. R., Vehkamäki, H., and Kirkby, J.: Molecular
    understanding of sulphuric acid–amine particle nucleation in the atmosphere, Nature,
    502, 359-363, 10.1038/nature12663, 2013.
Beck, L. J., Sarnela, N., Junninen, H., Hoppe, C. J. M., Garmash, O., Bianchi, F., Riva, M., Rose,
    C., Peräkylä, O., Wimmer, D., Kausiala, O., Jokinen, T., Ahonen, L., Mikkilä, J., Hakala,
    J., He, X.-C., Kontkanen, J., Wolf, K. K. E., Cappelletti, D., Mazzola, M., Traversi, R.,
    Petroselli, C., Viola, A. P., Vitale, V., Lange, R., Massling, A., Nøjgaard, J. K., Krejci,
    R., Karlsson, L., Zieger, P., Jang, S., Lee, K., Vakkari, V., Lampilahti, J., Thakur, R. C.,
    Leino, K., Kangasluoma, J., Duplissy, E.-M., Siivola, E., Marbouti, M., Tham, Y. J.,
    Saiz-Lopez, A., Petäjä, T., Ehn, M., Worsnop, D. R., Skov, H., Kulmala, M., Kerminen,
    V.-M., and Sipilä, M.: Differing Mechanisms of New Particle Formation at Two Arctic
    Sites, Geophysical Research Letters, 48, e2020GL091334,
    https://doi.org/10.1029/2020GL091334, 2021.
Benson, D. R., Markovich, A., Al-Refai, M., and Lee, S. H.: A Chemical Ionization Mass
    Spectrometer for ambient measurements of Ammonia, Atmos. Meas. Tech., 3, 1075-
    1087, 10.5194/amt-3-1075-2010, 2010.
Bianchi, F., Tröstl, J., Junninen, H., Frege, C., Henne, S., Hoyle, C. R., Molteni, U., Herrmann,
    E., Adamov, A., Bukowiecki, N., Chen, X., Duplissy, J., Gysel, M., Hutterli, M.,
    Kangasluoma, J., Kontkanen, J., Kürten, A., Manninen, H. E., Münch, S., Peräkylä, O.,
    Petäjä, T., Rondo, L., Williamson, C., Weingartner, E., Curtius, J., Worsnop, D. R.,
    Kulmala, M., Dommen, J., and Baltensperger, U.: New particle formation in the free
    troposphere: A question of chemistry and timing, Science, 352, 1109-1112,
    10.1126/science.aad5456, 2016.
Brean, J., Dall'Osto, M., Simó, R., Shi, Z., Beddows, D. C. S., and Harrison, R. M.: Open ocean
    and coastal new particle formation from sulfuric acid and amines around the Antarctic
    Peninsula, Nature Geoscience, 14, 383-388, 10.1038/s41561-021-00751-y, 2021.
Brean, J., Beddows, D. C. S., Shi, Z., Temime-Roussel, B., Marchand, N., Querol, X., Alastuey,
    A., Minguillón, M. C., and Harrison, R. M.: Molecular insights into new particle
    formation in Barcelona, Spain, Atmos. Chem. Phys., 20, 10029-10045, 10.5194/acp-20-
    10029-2020, 2020.
Cai, R., Yin, R., Li, X., Xie, H.-B., Yang, D., Kerminen, V.-M., Smith, J. N., Ma, Y., Hao, J.,
    Chen, J., Kulmala, M., Zheng, J., Jiang, J., and Elm, J.: Significant contributions of

trimethylamine to sulfuric acid nucleation in polluted environments, npj Climate and Atmospheric Science, 6, 75, 10.1038/s41612-023-00405-3, 2023.

Cai, R., Yan, C., Yang, D., Yin, R., Lu, Y., Deng, C., Fu, Y., Ruan, J., Li, X., Kontkanen, J., Zhang, Q., Kangasluoma, J., Ma, Y., Hao, J., Worsnop, D. R., Bianchi, F., Paasonen, P., Kerminen, V. M., Liu, Y., Wang, L., Zheng, J., Kulmala, M., and Jiang, J.: Sulfuric acid–amine nucleation in urban Beijing, Atmos. Chem. Phys., 21, 2457-2468, 10.5194/acp-21-2457-2021, 2021.

Chang, Y., Wang, H., Gao, Y., Jing, S. a., Lu, Y., Lou, S., Kuang, Y., Cheng, K., Ling, Q., Zhu, L., Tan, W., and Huang, R.-J.: Nonagricultural Emissions Dominate Urban Atmospheric Amines as Revealed by Mobile Measurements, Geophysical Research Letters, 49, e2021GL097640, https://doi.org/10.1029/2021GL097640, 2022.

Ellis, R. A., Murphy, J. G., Pattey, E., van Haarlem, R., O'Brien, J. M., and Herndon, S. C.: Characterizing a Quantum Cascade Tunable Infrared Laser Differential Absorption Spectrometer (QC-TILDAS) for measurements of atmospheric ammonia, Atmos. Meas. Tech., 3, 397-406, 10.5194/amt-3-397-2010, 2010.

Erupe, M. E., Viggiano, A. A., and Lee, S. H.: The effect of trimethylamine on atmospheric nucleation involving H_2SO_4, Atmos. Chem. Phys., 11, 4767-4775, 2011.

Erupe, M. E., Benson, D. R., Li, J., Young, L.-H., Verheggen, B., Al-Refai, M., Tahboub, O., Cunningham, V., Frimpong, F., Viggiano, A. A., and Lee, S.-H.: Correlation of aerosol nucleation rate with sulfuric acid and ammonia in Kent, Ohio: An atmospheric observation, Journal of Geophysical Research: Atmospheres, 115, https://doi.org/10.1029/2010JD013942, 2010.

Freshour, N. A., Carlson, K. K., Melka, Y. A., Hinz, S., Panta, B., and Hanson, D. R.: Amine permeation sources characterized with acid neutralization and sensitivies of an amine mass spectrometer, Atmos. Meas. Tech., 7, 3611-3621, 10.5194/amt-7-3611-2014, 2014.

Ge, X., Wexler, A. S., and Clegg, S. L.: Atmospheric amines – Part I. A review, Atmospheric Environment, 45, 524-546, https://doi.org/10.1016/j.atmosenv.2010.10.012, 2011a.

Ge, X., Wexler, A. S., and Clegg, S. L.: Atmospheric amines – Part II. Thermodynamic properties and gas/particle partitioning, Atmospheric Environment, 45, 561-577, https://doi.org/10.1016/j.atmosenv.2010.10.013, 2011b.

Glasoe, W. A., Volz, K., Panta, B., Freshour, N., Bachman, R., Hanson, D. R., McMurry, P. H., and Jen, C.: Sulfuric acid nucleation: an experimental study of the effect of seven bases, J. Geophys. Res., 120, 1933-1950, Doi: 10.1002/2014JD022730, 2015.

Griffith, D. W. T. and Galle, B.: Flux measurements of NH3, N2O and CO2 using dual beam FTIR spectroscopy and the flux–gradient technique, Atmospheric Environment, 34, 1087-1098, https://doi.org/10.1016/S1352-2310(99)00368-4, 2000.

Gu, B., Zhang, L., Van Dingenen, R., Vieno, M., Van Grinsven, H. J. M., Zhang, X., Zhang, S., Chen, Y., Wang, S., Ren, C., Rao, S., Holland, M., Winiwarter, W., Chen, D., Xu, J., and Sutton, M. A.: Abating ammonia is more cost-effective than nitrogen oxides for mitigating PM2.5 air pollution, Science, 374, 758-762, 10.1126/science.abf8623, 2021.

Hanson, D. R., McMurry, P. H., Jiang, J., Tanner, D., and Huey, L. G.: Ambient Pressure Proton Transfer Mass Spectrometry: Detection of Amines and Ammonia, Environmental Science & Technology, 45, 8881-8888, 10.1021/es201819a, 2011.

Jen, C. N., Bachman, R., Zhao, J., McMurry, P. H., and Hanson, D. R.: Diamine-sulfuric acid reactions are a potent source of new particle formation, Geophysical Research Letters, 43, 867-873, https://doi.org/10.1002/2015GL066958, 2016.

498   Jokinen, T., Sipilä, M., Kontkanen, J., Vakkari, V., Tisler, P., Duplissy, E. M., Junninen, H.,
499   Kangasluoma, J., Manninen, H. E., Petäjä, T., Kulmala, M., Worsnop, D. R., Kirkby, J.,
500   Virkkula, A., and Kerminen, V. M.: Ion-induced sulfuric acid–ammonia nucleation drives
501   particle formation in coastal Antarctica, Science Advances, 4, eaat9744,
502   10.1126/sciadv.aat9744,
503   Kanawade, V. P., Tripathi, S. N., Siingh, D., Gautam, A. S., Srivastava, A. K., Kamra, A. K.,
504   Soni, V. K., and Sethi, V.: Observations of new particle formation at two distinct Indian
505   subcontinental urban locations, Atmos. Environ., 96, 370-379, Doi:
506   10.1016/j.atmosenv.2014.08.001, 2014.
507   Köllner, F., Schneider, J., Willis, M. D., Klimach, T., Helleis, F., Bozem, H., Kunkel, D., Hoor,
508   P., Burkart, J., Leaitch, W. R., Aliabadi, A. A., Abbatt, J. P. D., Herber, A. B., and
509   Borrmann, S.: Particulate trimethylamine in the summertime Canadian high Arctic lower
510   troposphere, Atmos. Chem. Phys., 17, 13747-13766, 10.5194/acp-17-13747-2017, 2017.
511   Kürten, A., Bergen, A., Heinritzi, M., Leiminger, M., Lorenz, V., Piel, F., Simon, M., Sitals, R.,
512   Wagner, A. C., and Curtius, J.: Observation of new particle formation and measurement
513   of sulfuric acid, ammonia, amines and highly oxidized organic molecules at a rural site in
514   central Germany, Atmos. Chem. Phys., 16, 12793-12813, 10.5194/acp-16-12793-2016,
515   2016.
516   Lee, S.-H.: Perspective on the Recent Measurements of Reduced Nitrogen Compounds in the
517   Atmosphere, Frontiers in Environmental Science, 10, 10.3389/fenvs.2022.868534, 2022.
518   Lee, S.-H., Gordon, H., Yu, H., Lehtipalo, K., Haley, R., Li, Y., and Zhang, R.: New Particle
519   Formation in the Atmosphere: From Molecular Clusters to Global Climate, Journal of
520   Geophysical Research: Atmospheres, 124, 7098-7146, 10.1029/2018JD029356, 2019.
521   Leen, J. B., Yu, X.-Y., Gupta, M., Baer, D. S., Hubbe, J. M., Kluzek, C. D., Tomlinson, J. M.,
522   and Hubbell, M. R., II: Fast In Situ Airborne Measurement of Ammonia Using a Mid-
523   Infrared Off-Axis ICOS Spectrometer, Environmental Science & Technology, 47, 10446-
524   10453, 10.1021/es401134u, 2013.
525   Lehtipalo, K., Yan, C., Dada, L., Bianchi, F., Xiao, M., Wagner, R., Stolzenburg, D., Ahonen, L.
526   R., Amorim, A., Baccarini, A., Bauer, P. S., Baumgartner, B., Bergen, A., Bernhammer,
527   A.-K., Breitenlechner, M., Brilke, S., Buchholz, A., Mazon, S. B., Chen, D., Chen, X.,
528   Dias, A., Dommen, J., Draper, D. C., Duplissy, J., Ehn, M., Finkenzeller, H., Fischer, L.,
529   Frege, C., Fuchs, C., Garmash, O., Gordon, H., Hakala, J., He, X., Heikkinen, L.,
530   Heinritzi, M., Helm, J. C., Hofbauer, V., Hoyle, C. R., Jokinen, T., Kangasluoma, J.,
531   Kerminen, V.-M., Kim, C., Kirkby, J., Kontkanen, J., Kürten, A., Lawler, M. J., Mai, H.,
532   Mathot, S., Mauldin, R. L., Molteni, U., Nichman, L., Nie, W., Nieminen, T., Ojdanic,
533   A., Onnela, A., Passananti, M., Petäjä, T., Piel, F., Pospisilova, V., Quéléver, L. L. J.,
534   Rissanen, M. P., Rose, C., Sarnela, N., Schallhart, S., Schuchmann, S., Sengupta, K.,
535   Simon, M., Sipilä, M., Tauber, C., Tomé, A., Tröstl, J., Väisänen, O., Vogel, A. L.,
536   Volkamer, R., Wagner, A. C., Wang, M., Weitz, L., Wimmer, D., Ye, P., Ylisirniö, A.,
537   Zha, Q., Carslaw, K. S., Curtius, J., Donahue, N. M., Flagan, R. C., Hansel, A., Riipinen,
538   I., Virtanen, A., Winkler, P. M., Baltensperger, U., Kulmala, M., and Worsnop, D. R.:
539   Multicomponent new particle formation from sulfuric acid, ammonia, and biogenic
540   vapors, Science Advances, 4, eaau5363, 10.1126/sciadv.aau5363, 2018.
541   Liu, R., Liu, T., Huang, X., Ren, C., Wang, L., Niu, G., Yu, C., Zhang, Y., Wang, J., Qi, X., Nie,
542   W., Chi, X., and Ding, A.: Characteristics and sources of atmospheric ammonia at the

543   SORPES station in the western Yangtze river delta of China, Atmospheric Environment,
544   318, 120234, https://doi.org/10.1016/j.atmosenv.2023.120234, 2024.

545 Malloy, Q. G. J., Li, Q., Warren, B., Cocker Iii, D. R., Erupe, M. E., and Silva, P. J.: Secondary
546   organic aerosol formation from primary aliphatic amines with NO_3 radical,
547   Atmos. Chem. Phys., 9, 2051-2060, 10.5194/acp-9-2051-2009, 2009.

548 Mao, J., Yu, F., Zhang, Y., An, J., Wang, L., Zheng, J., Yao, L., Luo, G., Ma, W., Yu, Q.,
549   Huang, C., Li, L., and Chen, L.: High-resolution modeling of gaseous methylamines over
550   a polluted region in China: source-dependent emissions and implications of spatial
551   variations, Atmos. Chem. Phys., 18, 7933-7950, 10.5194/acp-18-7933-2018, 2018.

552 Martin, N. A., Ferracci, V., Cassidy, N., and Hoffnagle, J. A.: The application of a cavity ring-
553   down spectrometer to measurements of ambient ammonia using traceable primary
554   standard gas mixtures, Applied Physics B, 122, 219, 10.1007/s00340-016-6486-9, 2016.

555 McManus, J. B., Mark, S. Z., David, D. N., Jr., Joanne, H. S., Scott, C. H., Ezra, C. W., and
556   Rick, W.: Application of quantum cascade lasers to high-precision atmospheric trace gas
557   measurements, Optical Engineering, 49, 111124, 10.1117/1.3498782, 2010.

558 Miller, D. J., Sun, K., Tao, L., Khan, M. A., and Zondlo, M. A.: Open-path, quantum cascade-
559   laser-based sensor for high-resolution atmospheric ammonia measurements, Atmos.
560   Meas. Tech., 7, 81-93, 10.5194/amt-7-81-2014, 2014.

561 Myllys, N., Chee, S., Olenius, T., Lawler, M., and Smith, J.: Molecular-Level Understanding of
562   Synergistic Effects in Sulfuric Acid–Amine–Ammonia Mixed Clusters, The Journal of
563   Physical Chemistry A, 123, 2420-2425, 10.1021/acs.jpca.9b00909, 2019.

564 Nielsen, C. J.: Atmospheric Degradation of Amines (ADA). Summary report: Photo-oxidation of
565   methylamine, dimethylamine and trimethylamine. CLIMIT project no. 201604., Norge:
566   Norsk Institutt for Luftforskning, 2016.

567 Nielsen, C. J., Herrmann, H., and Weller, C.: Atmospheric chemistry and environmental impact
568   of the use of amines in carbon capture and storage (CCS), Chemical Society Reviews, 41,
569   6684-6704, 10.1039/C2CS35059A, 2012.

570 Nowak, J. B., Neuman, J. A., Bahreini, R., Brock, C. A., Middlebrook, A. M., Wollny, A. G.,
571   Holloway, J. S., Peischl, J., Ryerson, T. B., and Fehsenfeld, F. C.: Airborne observations
572   of ammonia and ammonium nitrate formation over Houston, Texas, Journal of
573   Geophysical Research: Atmospheres, 115, https://doi.org/10.1029/2010JD014195, 2010.

574 Nowak, J. B., Huey, L. G., Russell, A. G., Tian, D., Neuman, J. A., Orsini, D., Sjostedt, S. J.,
575   Sullivan, A. P., Tanner, D. J., Weber, R. J., Nenes, A., Edgerton, E., and Fehsenfeld, F.
576   C.: Analysis of urban gas phase ammonia measurements from the 2002 Atlanta Aerosol
577   Nucleation and Real-Time Characterization Experiment (ANARChE), Journal of
578   Geophysical Research: Atmospheres, 111, https://doi.org/10.1029/2006JD007113, 2006.

579 Petrus, M., Popa, C., and Bratu, A. M.: Ammonia Concentration in Ambient Air in a Peri-Urban
580   Area Using a Laser Photoacoustic Spectroscopy Detector, Materials (Basel), 15,
581   10.3390/ma15093182, 2022.

582 Pollack, I. B., Lindaas, J., Roscioli, J. R., Agnese, M., Permar, W., Hu, L., and Fischer, E. V.:
583   Evaluation of ambient ammonia measurements from a research aircraft using a closed-
584   path QC-TILDAS operated with active continuous passivation, Atmos. Meas. Tech., 12,
585   3717-3742, 10.5194/amt-12-3717-2019, 2019.

586 Pushkarsky, M. B., Webber, M. E., Baghdassarian, O., Narasimhan, L. R., and Patel, C. K. N.:
587   Laser-based photoacoustic ammonia sensors for industrial applications, Applied Physics
588   B, 75, 391-396, 10.1007/s00340-002-0967-8, 2002.

Qiu, C. and Zhang, R.: Multiphase chemistry of atmospheric amines, Physical Chemistry Chemical Physics, 15, 5738-5752, 10.1039/C3CP43446J, 2013.

Schwab, J. J., Li, Y., Bae, M. S., Demerjian, K. L., Hou, J., Zhou, X., Jensen, B., and Pryor, S. C.: A laboratory intercomparison of real-time gaseous ammonia measurement methods, Environ Sci Technol, 41, 8412-8419, 10.1021/es070354r, 2007.

Silva, P. J., Erupe, M. E., Price, D., Elias, J., G. J. Malloy, Q., Li, Q., Warren, B., and Cocker, D. R., III: Trimethylamine as Precursor to Secondary Organic Aerosol Formation via Nitrate Radical Reaction in the Atmosphere, Environmental Science & Technology, 42, 4689-4696, 10.1021/es703016v, 2008.

Smith, J. N., Barsanti, K. C., Friedli, H. R., Ehn, M., Kulmala, M., Collins, D. R., Scheckman, J. H., Williams, B. J., and McMurry, P. H.: Observations of aminium salts in atmospheric nanoparticles and possible climatic implications, Proc. Natl. Acad. Sci., 107, 6634-6639, 2010.

Wang, G., Zhang, R., Gomez, M. E., Yang, L., Levy Zamora, M., Hu, M., Lin, Y., Peng, J., Guo, S., Meng, J., Li, J., Cheng, C., Hu, T., Ren, Y., Wang, Y., Gao, J., Cao, J., An, Z., Zhou, W., Li, G., Wang, J., Tian, P., Marrero-Ortiz, W., Secrest, J., Du, Z., Zheng, J., Shang, D., Zeng, L., Shao, M., Wang, W., Huang, Y., Wang, Y., Zhu, Y., Li, Y., Hu, J., Pan, B., Cai, L., Cheng, Y., Ji, Y., Zhang, F., Rosenfeld, D., Liss, P. S., Duce, R. A., Kolb, C. E., and Molina, M. J.: Persistent sulfate formation from London Fog to Chinese haze, Proceedings of the National Academy of Sciences, 113, 13630-13635, 10.1073/pnas.1616540113, 2016.

Wang, M., Kong, W., Marten, R., He, X.-C., Chen, D., Pfeifer, J., Heitto, A., Kontkanen, J., Dada, L., Kürten, A., Yli-Juuti, T., Manninen, H. E., Amanatidis, S., Amorim, A., Baalbaki, R., Baccarini, A., Bell, D. M., Bertozzi, B., Bräkling, S., Brilke, S., Murillo, L. C., Chiu, R., Chu, B., De Menezes, L.-P., Duplissy, J., Finkenzeller, H., Carracedo, L. G., Granzin, M., Guida, R., Hansel, A., Hofbauer, V., Krechmer, J., Lehtipalo, K., Lamkaddam, H., Lampimäki, M., Lee, C. P., Makhmutov, V., Marie, G., Mathot, S., Mauldin, R. L., Mentler, B., Müller, T., Onnela, A., Partoll, E., Petäjä, T., Philippov, M., Pospisilova, V., Ranjithkumar, A., Rissanen, M., Rörup, B., Scholz, W., Shen, J., Simon, M., Sipilä, M., Steiner, G., Stolzenburg, D., Tham, Y. J., Tomé, A., Wagner, A. C., Wang, D. S., Wang, Y., Weber, S. K., Winkler, P. M., Wlasits, P. J., Wu, Y., Xiao, M., Ye, Q., Zauner-Wieczorek, M., Zhou, X., Volkamer, R., Riipinen, I., Dommen, J., Curtius, J., Baltensperger, U., Kulmala, M., Worsnop, D. R., Kirkby, J., Seinfeld, J. H., El-Haddad, I., Flagan, R. C., and Donahue, N. M.: Rapid growth of new atmospheric particles by nitric acid and ammonia condensation, Nature, 581, 184-189, 10.1038/s41586-020-2270-4, 2020a.

Wang, Y., Yang, G., Lu, Y., Liu, Y., Chen, J., and Wang, L.: Detection of gaseous dimethylamine using vocus proton-transfer-reaction time-of-flight mass spectrometry, Atmospheric Environment, 243, 117875, https://doi.org/10.1016/j.atmosenv.2020.117875, 2020b.

Xiao, M., Hoyle, C. R., Dada, L., Stolzenburg, D., Kürten, A., Wang, M., Lamkaddam, H., Garmash, O., Mentler, B., Molteni, U., Baccarini, A., Simon, M., He, X. C., Lehtipalo, K., Ahonen, L. R., Baalbaki, R., Bauer, P. S., Beck, L., Bell, D., Bianchi, F., Brilke, S., Chen, D., Chiu, R., Dias, A., Duplissy, J., Finkenzeller, H., Gordon, H., Hofbauer, V., Kim, C., Koenig, T. K., Lampilahti, J., Lee, C. P., Li, Z., Mai, H., Makhmutov, V., Manninen, H. E., Marten, R., Mathot, S., Mauldin, R. L., Nie, W., Onnela, A., Partoll, E.,

Petäjä, T., Pfeifer, J., Pospisilova, V., Quéléver, L. L. J., Rissanen, M., Schobesberger, S., Schuchmann, S., Stozhkov, Y., Tauber, C., Tham, Y. J., Tomé, A., Vazquez-Pufleau, M., Wagner, A. C., Wagner, R., Wang, Y., Weitz, L., Wimmer, D., Wu, Y., Yan, C., Ye, P., Ye, Q., Zha, Q., Zhou, X., Amorim, A., Carslaw, K., Curtius, J., Hansel, A., Volkamer, R., Winkler, P. M., Flagan, R. C., Kulmala, M., Worsnop, D. R., Kirkby, J., Donahue, N. M., Baltensperger, U., El Haddad, I., and Dommen, J.: The driving factors of new particle formation and growth in the polluted boundary layer, Atmos. Chem. Phys., 21, 14275-14291, 10.5194/acp-21-14275-2021, 2021.

Xiao, S., Wang, M. Y., Yao, L., Kulmala, M., Zhou, B., Yang, X., Chen, J. M., Wang, D. F., Fu, Q. Y., Worsnop, D. R., and Wang, L.: Strong atmospheric new particle formation in winter in urban Shanghai, China, Atmos. Chem. Phys., 15, 1769-1781, 10.5194/acp-15-1769-2015, 2015.

Yan, C., Yin, R., Lu, Y., Dada, L., Yang, D., Fu, Y., Kontkanen, J., Deng, C., Garmash, O., Ruan, J., Baalbaki, R., Schervish, M., Cai, R., Bloss, M., Chan, T., Chen, T., Chen, Q., Chen, X., Chen, Y., Chu, B., Dällenbach, K., Foreback, B., He, X., Heikkinen, L., Jokinen, T., Junninen, H., Kangasluoma, J., Kokkonen, T., Kurppa, M., Lehtipalo, K., Li, H., Li, H., Li, X., Liu, Y., Ma, Q., Paasonen, P., Rantala, P., Pileci, R. E., Rusanen, A., Sarnela, N., Simonen, P., Wang, S., Wang, W., Wang, Y., Xue, M., Yang, G., Yao, L., Zhou, Y., Kujansuu, J., Petäjä, T., Nie, W., Ma, Y., Ge, M., He, H., Donahue, N. M., Worsnop, D. R., Veli-Matti, K., Wang, L., Liu, Y., Zheng, J., Kulmala, M., Jiang, J., and Bianchi, F.: The Synergistic Role of Sulfuric Acid, Bases, and Oxidized Organics Governing New-Particle Formation in Beijing, Geophysical Research Letters, 48, e2020GL091944, https://doi.org/10.1029/2020GL091944, 2021.

Yao, L., Wang, M. Y., Wang, X. K., Liu, Y. J., Chen, H. F., Zheng, J., Nie, W., Ding, A. J., Geng, F. H., Wang, D. F., Chen, J. M., Worsnop, D. R., and Wang, L.: Detection of atmospheric gaseous amines and amides by a high-resolution time-of-flight chemical ionization mass spectrometer with protonated ethanol reagent ions, Atmos. Chem. Phys., 16, 14527-14543, 10.5194/acp-16-14527-2016, 2016.

You, Y., Kanawade, V. P., de Gouw, J. A., Guenther, A. B., Madronich, S., Sierra-Hernández, M. R., Lawler, M., Smith, J. N., Takahama, S., Ruggeri, G., Koss, A., Olson, K., Baumann, K., Weber, R. J., Nenes, A., Guo, H., Edgerton, E. S., Porcelli, L., Brune, W. H., Goldstein, A. H., and Lee, S. H.: Atmospheric amines and ammonia measured with a Chemical Ionization Mass Spectrometer (CIMS), Atmos. Chem. Phys. , 14, 12181-12194, Doi: 10.5194/acpd-14-16411-2014, 2014.

Yu, H. and Lee, S. H.: A chemical ionization mass spectrometer for the detection of atmospheric amines, Environ. Chem., 9, 190-201, 2012

Yu, H., McGraw, R., and Lee, S. H.: Effects of amines on formation of sub-3 nm particles and their subsequent growth, Geophys. Res. Lett., 39, Doi: 10.1029/2011gl050099, 10.1029/2011gl050099, 2012.

Zhao, B., Donahue, N. M., Zhang, K., Mao, L., Shrivastava, M., Ma, P.-L., Shen, J., Wang, S., Sun, J., Gordon, H., Tang, S., Fast, J., Wang, M., Gao, Y., Yan, C., Singh, B., Li, Z., Huang, L., Lou, S., Lin, G., Wang, H., Jiang, J., Ding, A., Nie, W., Qi, X., Chi, X., and Wang, L.: Global variability in atmospheric new particle formation mechanisms, Nature, 631, 98-105, 10.1038/s41586-024-07547-1, 2024.

Zheng, J., Ma, Y., Chen, M., Zhang, Q., Wang, L., Khalizov, A. F., Yao, L., Wang, Z., Wang, X., and Chen, L.: Measurement of atmospheric amines and ammonia using the high

681   resolution time-of-flight chemical ionization mass spectrometry, Atmospheric

682   Environment, 102, 249-259, https://doi.org/10.1016/j.atmosenv.2014.12.002, 2015.

683 Zhu, S., Yan, C., Zheng, J., Chen, C., Ning, H., Yang, D., Wang, M., Ma, Y., Zhan, J., Hua, C.,

684   Yin, R., Li, Y., Liu, Y., Jiang, J., Yao, L., Wang, L., Kulmala, M., and Worsnop, D. R.:

685   Observation and Source Apportionment of Atmospheric Alkaline Gases in Urban

686   Beijing, Environmental Science & Technology, 56, 17545-17555,

687   10.1021/acs.est.2c03584, 2022.

688